Transition metal-free synthesis of 2-aryl quinazolines via alcohol dehydrogenation

Hima P [a], Vageesh M [a], Michele Tomasini [b,c], Albert Poater [c,*], Raju Dey [a,*]

[a] *Department of Chemistry, National Institute of Technology Calicut, Kozhikode, 673601, India*
[b] *Department of Chemistry and Biology, Università di Salerno, Via Ponte don Melillo, 84084, Fisciano, Italy*
[c] *Institut de Química Computacional i Catàlisi, Departament de Química, Universitat de Girona, c/ Mª Aurèlia Capmany 69, 17003 Girona, Catalonia, Spain*

ARTICLE INFO

ABSTRACT

We report here a transition metal-free synthesis of quinazoline derivatives starting from 2-aminobenzyl alcohols and aryl amides via an alcohol dehydrogenation strategy promoted by potassium tertiary butoxide. The control experiments are carried out to identify the reaction intermediates and the role of the K^+ ion in the reaction. The DFT calculations unveil the reaction mechanism, with special focus on the rate determining state. The present method tolerates a variety of functional groups providing easy access to diversely substituted quinazolines.

1. Introduction

Quinazolines are a class of nitrogen-containing heterocyclic compounds [1], that are widely found in natural products [2] and used in pharmaceutical industries (Fig. 1), particularly as anti-bacterial [3], anti-fungal [4], anti-inflammatory [5], antimalarial [6], anti-tumor [7], anti-viral [8], anti-tuberculosis [9], anti-hypertension [10], anti-obesity [11], anti-psychotic [12], anti-diabetic [13] agent. Additionally, their inhibitory effects on thymidylate synthase [14], poly-(ADP-ribose) polymerase (PARP) [15], and tyrosine kinase [16] are well documented. Several quinazoline derivatives are used as approved drugs, for instance, prazosin hydrochloride, doxazosin mesylate, and terazosin hydrochloride [17]. Thus, with significant biological activities, quinazoline derivatives have received the utmost importance in organic synthesis and medicinal chemistry research.

In recent years, several procedures have been developed for the synthesis of quinazoline derivatives. Most of the methods are based on either oxidative condensation or coupling reactions [18–27]. However, they are associated with severe drawbacks, such as the use of chemically unstable o-aminobenzaldehyde as the reactant [28], more than stoichiometric amounts of hazardous oxidants [29], generation of a large quantity of hazardous waste [30], etc. Thus, an efficient method, using benign chemicals under eco-friendly mild reaction conditions and without producing much waste, is well appreciated.

In this context, acceptorless dehydrogenative coupling (ADC) reactions have emerged as an efficient tool for synthesizing diverse heterocyclic compounds [31,32], from relatively inexpensive and readily available starting materials [33,34]. The only by-products generated in this type of reaction are hydrogen and water [35–37], which makes the strategy environmentally benign. One prominent example in this category is the dehydrogenation of alcohols followed by coupling with a suitable reagent [38]. The above strategy has been extended for the synthesis of substituted quinazoline derivatives (see Scheme 1) by several research groups. For example, Paul and coworkers disclosed the synthesis of aryl quinazoline by nickel-catalyzed alcohol dehydrogenation followed by condensation with 2-aminobenzylamine [39]. In similar reports, Balaraman and co-workers revealed the synthesis of quinazoline using 2-aminobenzyl alcohol and amides as reactants and the manganese pincer complex as a catalyst in the presence of 0.4 equivalents of potassium-tert-butoxide (KO^{t}Bu) [40].

In general, 2-aminobenzyl alcohols are found to undergo alcohol dehydrogenation to form 2-amino benzaldehyde as an intermediate that coupled with amide [40] or nitrile [41–43], resulting in the formation of quinazoline derivatives. In another report, Li and coworkers showed that iron and phenanthroline catalyst systems combined with CsOH·H$_2$O as a base could be used for the same transformation [44].

Despite economic, environmental, and operational benefits, acceptorless dehydrogenative coupling reactions mainly depend on the use of transition metals e.g., Mn [45–49], Fe [50,51], Ni [52–54], Co [55–59], Ir [60–63], Ag [64], Rh [65], Ru [66,67], Os [68], or Pt [69], as the catalysts. In addition to that, the requirement of an expensive and hazardous ligand system [70], prolonged reaction time, and low yield of

---

* Corresponding authors.

E-mail addresses: albert.poater@udg.edu (A. Poater), rajudey@nitc.ac.in (R. Dey).
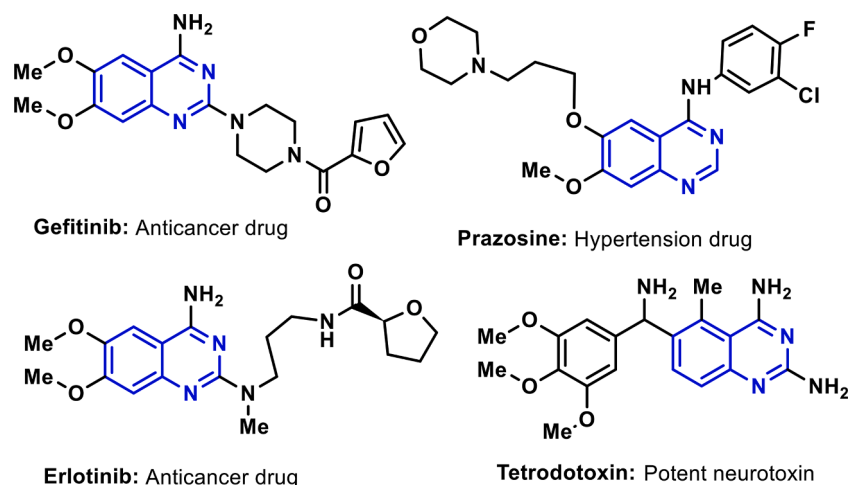
Fig. 1. Selected Examples of Pharmaceutically Important Quinazoline Containing Molecules.

Scheme 1. Synthesis of Quinazoline Using Alcohol Dehydrogenation Method.
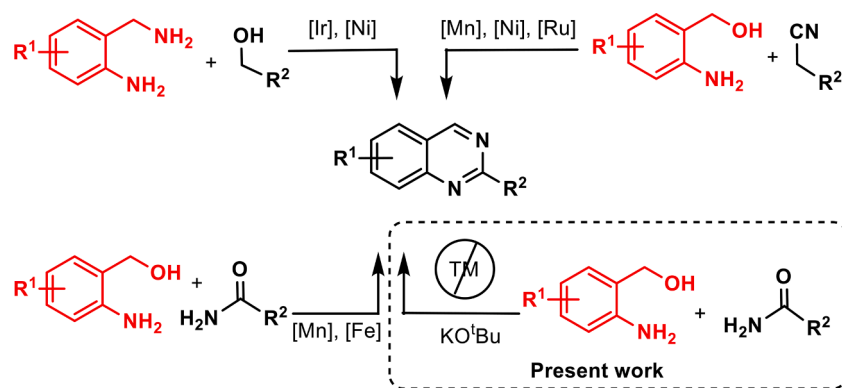
products are the other limitations [71].

The use of heavy transition metals in organic reactions have posed some serious limitations as many of these metals are in general hazardous to the environment, expensive, and scarce in nature [72,73]. Similarly, the ligands used in these reactions are generally difficult to prepare and expensive. Moreover, metal and ligand contamination especially in pharmaceutical products are closely regulated. Hence, transition metal-free protocols are gaining tremendous importance in overcoming these challenges [74–76]. The base-mediated β-alkylation of alcohols in aerobic conditions is well known [77]. In line with heterogeneous bases have been demonstrated as catalysts for dehydrogenative processes [78–81], the use of potassium-tert-butoxide in dehydrogenation is not new and was reported by Grubbs and coworkers in the silylation of C—H bonds in aromatic heterocycles [82]. Later Yu and his group disclosed potassium tert-butoxide-promoted acceptorless dehydrogenation of N-heterocycles [83]. Recently potassium-tert-butoxide mediated direct synthesis of amides from alcohol was reported by Fang and co-workers via an MPV-type hydrogen transfer process [84]. Thus, to overcome the aforementioned challenges involved in transition metal catalysis and to meet the requirement of improved transition metal free protocols in heterocyclic chemistry [85–94], we report here a simple and straightforward method for synthesizing 2-arylquinazoline derivatives by dehydrogenative coupling between 2-aminobenzyl alcohol and an amide in the presence of K^{t}OBu. The experimental procedure is very simple and straightforward, does not involve any transition metal catalyst [95]. A mixture of 2-aminobenzyl alcohol and benzamide in t-amyl alcohol was stirred at 100 °C in the presence of K^{t}OBu for a required period of time (TLC). Standard workup and

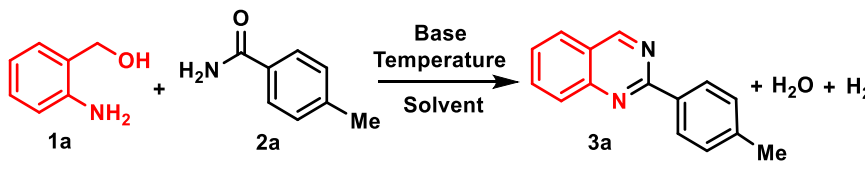purification by column chromatography afforded the product.

2. Experimental section

General procedures for the synthesis of quinazoline. A mixture of aryl amide (0.5 mmol), 2-aminobenzyl alcohol (0.75 mmol), and KO^{t}Bu (1.0 mmol) in 2 mL t-amyl alcohol was heated at 100 °C under argon atmosphere for 16 h in a preheated heating block. After completion of the reaction, the reaction vessel was cooled to room temperature and diluted with 10 mL ethyl acetate. The reaction mixture was then filtered using celite. The filtrate was dried using a rotary evaporator, volatile impurities were removed under vacuum, and further purification of the product had been carried out by column chromatography using silica gel as stationary phase and hexane and ethyl acetate as eluent. The purified products are characterized by IR and ^{1}H NMR and ^{13}C NMR spectroscopy.

2-(p-tolyl)quinazoline (**3a**, Table 2). Eluent: Hexane/Ethyl acetate (25:1), Yellow solid (91%); IR (KBr) 1548, 1557, 1480, 1382, 1012, 833, 790, 729 cm^{-1}; ^{1}H NMR (500 MHz, CDCl$_3$) δ 9.34 (s, 1H), 8.43 (d, $J =$ 8.2 Hz, 2H), 7.99 (d, $J = 8.4$ Hz, 1H), 7.80–7.77 (m, 2H), 7.48 (t, $J = 7.4$ Hz, 1H), 7.26–7.16 (m, 2H), 2.35 (s, 3H); ^{13}C NMR (125 MHz, CDCl$_3$) δ 161.2, 160.6, 150.8, 141.0, 135.3, 134.2, 129.5, 128.7, 128.6, 127.2, 127.3, 123.6, 21.6.

2-(4-chlorophenyl)quinazoline (**3b**, Table 2). Eluent: Hexane/Ethyl acetate (20:1), Yellow solid (83%); IR (KBr) 1549, 1494, 1411, 1087, 1005, 853, 792, 722, 457 cm^{-1}; ^{1}H NMR (500 MHz, CDCl$_3$) δ 9.36 (s, 1H), 8.49 (dt, $J = 9.0$, 2.2 Hz, 2H), 8.01–7.99 (m, 1H), 7.85–7.81 (m, 2H), 7.55–7.52 (m, 1H), 7.41 (dt, $J = 9.1$, 2.1 Hz, 2H); ^{13}C NMR (125

Table 1
Optimization of the Reaction Conditions.

Entry	Solvent	Base	Temperature (^{o}C)	Time (h)	Yield(3a)[b] (%)
1	Toluene	^{t}BuOK	100	16	77
2	t-amyl alcohol	^{t}BuOK	100	16	99
3	t-amyl alcohol	^{t}BuOK	100	8	47
4	t-amyl alcohol	^{t}BuOK	100	12	75
5	DMF	^{t}BuOK	100	16	21
6	H_2O	^{t}BuOK	100	16	No reaction
7	t-amyl alcohol	^{t}BuOK	rt	16	Trace amount
8	t-amyl alcohol	^{t}BuOK	80	16	24
9	t-amyl alcohol	KOH	100	16	50
10	t-amyl alcohol	Cs_2CO_3	100	16	28
11	t-amyl alcohol	K_2CO_3	100	16	No reaction
12	t-amyl alcohol	NaOH	100	16	Trace amount

[a] Reaction conditions: 2-aminobenzyl alcohol (0.75 mmol), amide (0.5 mmol), base (1 mmol), solvent (2 mL), under Ar. [b] Yield was calculated by NMR spectroscopy using 1,4 dimethoxybenzene as the internal standard.

MHz, CDCl$_3$) δ 160.4, 159.9, 150.5, 136.8, 136.4, 134.2, 129.8, 128.7, 128.5, 127.4, 127.1, 123.5.

2-(2,4-dichlorophenyl)quinazoline (**3c,** Table 2). Eluent: Hexane/ Ethyl acetate (10:1), Yellow solid (72%); IR (KBr) 1531, 1491, 1409, 1376, 840, 772, 451 cm^{-1}; ^{1}H NMR (500 MHz, CDCl$_3$) δ 9.45 (s, 1H), 8.05 (d, $J = 8.4$ Hz, 1H), 7.91 (t, $J = 8.5$ Hz, 2H), 7.74 (d, $J = 8.4$ Hz, 1H), 7.64 (s, 1H), 7.49 (d, $J = 1.7$ Hz, 1H), 7.33 (dd, $J = 8.2, 1.7$ Hz, 1H); ^{13}C NMR (125 MHz, CDCl$_3$) δ 160.7, 160.3, 150.2, 135.8, 135.7, 134.7, 133.9, 132.8, 130.4, 128.5, 128.4, 127.2, 127.1, 123.2, 77.2, 77.0, 76.7.

2-(2-chlorophenyl)quinazoline (**3d,** Table 2). Eluent: Hexane/Ethyl acetate (20:1), Yellow solid (72%); IR(KBr) 1535, 1385, 1035, 948, 764, 719 cm^{-1}; ^{1}H NMR (500 MHz, CDCl$_3$) δ 9.50 (s, 1H), 8.10 (d, $J = 8.6$ Hz, 1H), 7.96–7.91 (m, 2H), 7.78–7.76 (m, 1H), 7.68–7.64 (m, 1H), 7.49–7.47 (m, 1H), 7.35 (dt, $J = 4.8, 2.2$ Hz, 2H); ^{13}C NMR (125 MHz, CDCl$_3$) δ 161.9, 160.2, 150.2, 138.2, 134.3, 132.8, 131.7, 130.5, 130.3, 128.5, 128.0, 127.1, 126.8, 123.2.

2-(3-bromophenyl)quinazoline (**3e,** Table 2). Eluent: Hexane/Ethyl acetate (20:1), Yellow solid (86%); IR (KBr) 1549, 1494, 1100, 1005, 849, 792, 722 cm^{-1}; ^{1}H NMR (500 MHz, CDCl$_3$) δ 9.40 (s, 1H), 8.73 (t, $J = 1.8$ Hz, 1H), 8.49 (dd, $J = 7.8, 1.1$ Hz, 1H), 8.03 (d, $J = 8.4$ Hz, 1H), 7.89–7.86 (m, 2H), 7.59–7.55 (m, 2H), 7.34 (t, $J = 7.8$ Hz, 1H); ^{13}C NMR (125 MHz, CDCl$_3$) δ 160.6, 159.6, 150.7, 140.1, 134.3, 133.5, 131.6, 130.1, 128.7, 127.7, 127.2, 127.1, 123.7, 122.9.

2-(4-bromophenyl)quinazoline (**3f,** Table 2). Eluent: Hexane/Ethyl acetate (20:1), Yellow solid (81%); IR (KBr) 1555, 1549, 1489, 1100, 1005, 849, 790 cm^{-1}; ^{1}H NMR (500 MHz, CDCl$_3$) δ 9.37 (s, 1H), 8.43 (dd, $J = 6.8, 2.0$ Hz, 2H), 8.00 (dd, $J = 8.4, 1.0$ Hz, 1H), 7.86–7.83 (m, 2H), 7.60–7.55 (m, 3H); ^{13}C NMR (125 MHz, CDCl$_3$) δ 160.5, 160.1, 150.7, 137.0, 134.3, 131.8, 130.1, 128.6, 127.5, 127.2, 125.4, 123.6

2-phenylquinazoline (**3g,** Table 2). Eluent: Hexane/Ethyl acetate (25:1), Yellow solid (93%); IR (KBr), 1617, 1578, 1546, 1480, 1442, 1382, 778, 701 cm^{-1} .^{1}H NMR (500 MHz, CDCl$_3$) δ 9.39 (s, 1H), 8.55–8.53 (m, 2H), 8.02 (d, $J = 8.6$ Hz, 1H), 7.85–7.81 (m, 2H), 7.53 (t, $J = 7.4$ Hz, 1H), 7.48–7.41 (m, 3H). ^{13}C NMR (125 MHz, CDCl$_3$) δ 161.0, 160.6, 150.8, 138.0, 134.3, 130.8, 128.7, 128.8, 127.4, 127.2, 123.6.

2-(p-methoxyphenyl)quinazoline (**3h,** Table 2). Eluent: Hexane/Ethyl acetate (10:1), Yellow solid (91%); IR (KBr) 1549, 1407, 1327, 1242, 1046, 805, 788 cm^{-1}; ^{1}H NMR (500 MHz, CDCl$_3$) δ 9.33 (s, 1H), 8.50 (dd, $J = 6.9, 2.1$ Hz, 2H), 7.96 (dd, $J = 8.4, 0.8$ Hz, 1H), 7.81–7.77 (m, 2H), 7.50–7.47 (m, 1H), 6.97 (dd, $J = 6.9, 2.1$ Hz, 2H), 3.82 (s, 3H); ^{13}C

Table 2
Substrate Scope.
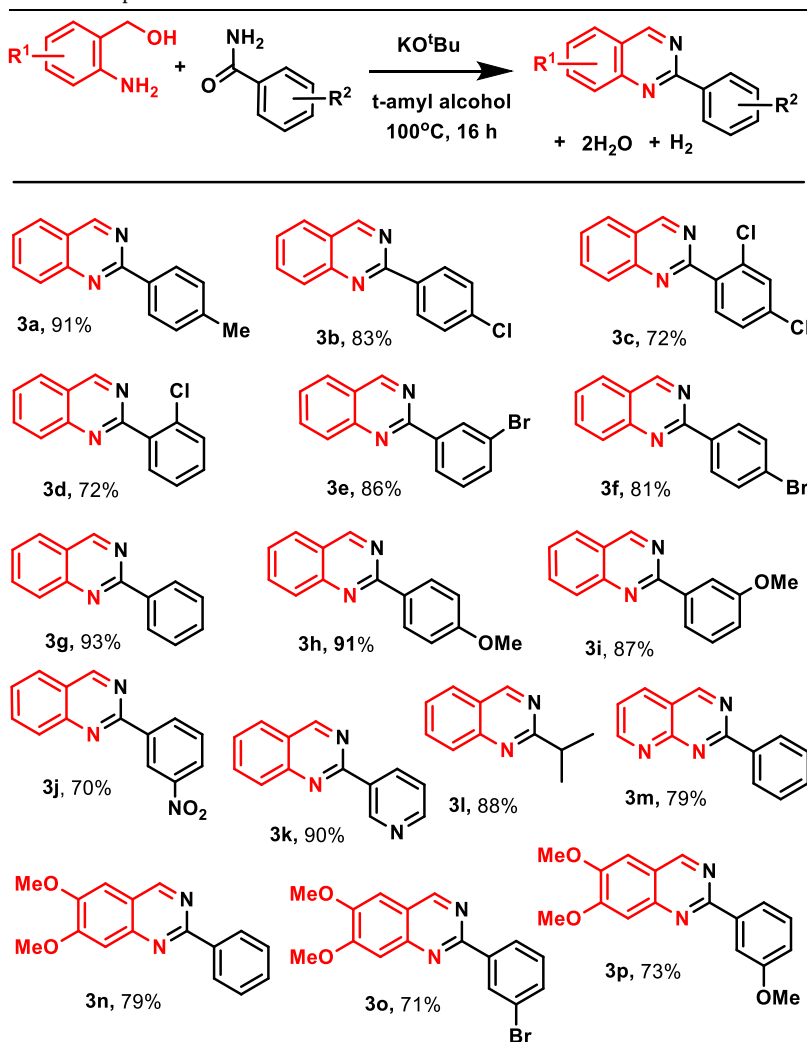
^{a}Reaction conditions: 2-aminobenzyl alcohol (0.75 mmol), amide (0.5 mmol), base (1 mmol), solvent (2 ml), at 100 °C under Ar for 16 h. ^{b} Yields refer to those of pure products characterized by IR. ^{1}H NMR, and ^{13}C NMR spectroscopic data.

NMR (125 MHz, CDCl$_3$) δ 161.8, 160.9, 160.4, 150.8, 134.0, 130.7, 130.2, 128.4, 127.1, 126.8, 123.3, 114.0, 55.4.

2-(3-methoxyphenyl)quinazoline (**3i**, Table 2). Eluent: Hexane/Ethyl acetate (10:1), White solid (87%); IR(KBr) 1546, 1407, 1328, 1242, 1046, 805 cm^{-1}; ^{1}H NMR (500 MHz, CDCl$_3$) δ 9.33 (s, 1H), 8.51–8.48 (m, 2H), 7.96 (dd, *J* = 8.4, 0.8 Hz, 1H), 7.81–7.77 (m, 2H), 7.50–7.47 (m, 1H), 6.98–6.95 (m, 2H), 3.82 (s, 3H); ^{13}C NMR (125 MHz, CDCl$_3$) δ 160.5, 160.3, 159.9, 150.4, 139.1, 134.2, 129.5, 128.4, 127.3, 127.0, 123.5, 121.1, 117.2, 112.9, 55.3.

2-(3-nitrophenyl)quinazoline (**3j**, Table 2). Eluent: Hexane/Ethyl acetate (5:1), Yellow solid (70%); IR(KBr) 1554, 1390, 1199, 1046, 722 cm^{-1}; ^{1}H NMR (500 MHz, CDCl$_3$) δ 9.44 (t, *J* = 2.1 Hz, 2H), 8.92–8.90 (m, 1H), 8.28 (dq, *J* = 8.2, 1.1 Hz, 1H), 8.07 (d, *J* = 8.4 Hz, 1H), 7.92–7.89 (m, 2H), 7.65–7.61 (m, 2H); ^{13}C NMR (125 MHz, CDCl$_3$) δ 175.8, 175.3, 159.8, 157.7, 149.6, 147.9, 138.9, 133.6, 133.2, 128.5, 127.8, 127.1, 126.2, 124.0, 123.0, 122.6.

2-(pyridin-3-yl)quinazoline (**3k**, Table 2). Eluent: Hexane/Ethyl acetate (4:1), Orange solid (90%); IR(KBr) 3277, 1614, 1569, 1484, 805, 694 cm^{-1}; ^{1}H NMR (500 MHz, CDCl$_3$) δ 9.70 (s, 1H), 9.33 (s, 1H), 8.75 (d, *J* = 7.8 Hz, 1H), 8.62 (d, *J* = 3.8 Hz, 1H), 7.96 (d, *J* = 8.8 Hz, 1H), 7.82–7.79 (m, 2H), 7.52 (t, *J* = 7.4 Hz, 1H), 7.35 (dd, *J* = 7.6, 4.8 Hz, 1H); ^{13}C NMR (125 MHz, CDCl$_3$) δ 159.6, 157.9, 149.7, 149.5, 148.8,

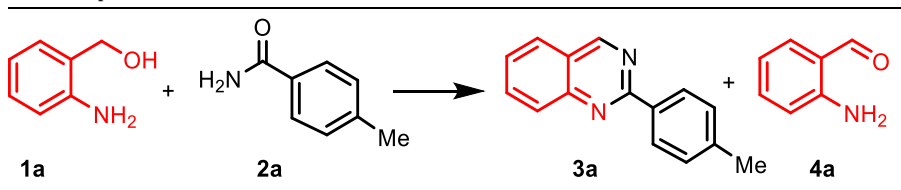135.0, 133.4, 132.6, 127.5, 126.8, 126.1, 122.7, 122.5.

2-isopropylquinazoline (**3l**, Table 2). Eluent: Hexane/Ethyl acetate (20:1), Yellow viscous liquid (88%); IR (KBr) 2954, 1614, 1580, 1494, 1415, 764, 609 cm^{-1}; ^{1}H NMR (500 MHz, CDCl$_3$) δ 9.29 (s, 1H), 7.93 (d, *J* = 8.6 Hz, 1H), 7.80 (t, *J* = 8.3 Hz, 2H), 7.51 (t, *J* = 7.4 Hz, 1H), 3.35–3.30 (m, 1H), 1.38–1.33 (m, 6H); ^{13}C NMR (125 MHz, CDCl$_3$) δ 171.7, 160.6, 150.3, 134.1, 128.0, 127.2, 127.0, 123.3, 38.0, 21.9.

2-phenylpyrido[2,3-d] pyrimidine (**3m**, Table 2). Eluent: Hexane/ Ethyl acetate (4:1), Yellow solid (79%); IR (KBr) 1614, 1569, 1484, 1478, 800, 708 cm^{-1}; ^{1}H NMR (500 MHz, CDCl$_3$) δ 9.47 (s, 1H), 9.21 (d, *J* = 2.1 Hz, 1H), 8.68–8.66 (m, 2H), 8.26 (dd, *J* = 8.0, 1.9 Hz, 1H), 7.76–7.74 (m, 1H), 7.48–7.44 (m, 3H), 7.37 (t, *J* = 7.8 Hz, 1H); ^{13}C NMR (125 MHz, CDCl$_3$) δ 157.2, 148.1, 139.5, 136.7, 129.6, 129.2, 128.7, 127.5, 127.4, 126.2, 118.9.

6,7-dimethoxy-2-phenylquinazoline (**3n**, Table 2). Eluent: Hexane/ Ethyl acetate (10:1), Yellow solid (79%); IR (KBr) 1545, 1409, 1325, 1239, 1046, 805 cm^{-1}; ^{1}H NMR (500 MHz, CDCl$_3$) δ 9.08 (s, 1H), 8.40–8.38 (m, 2H), 7.36–7.32 (m, 3H), 7.26 (s, 1H), 6.97 (s, 1H), 3.93 (s, 3H), 3.89 (s, 3H); ^{13}C NMR (125 MHz, CDCl$_3$) δ 159.9, 156.9, 156.8, 150.7, 149.1, 137.6, 130.6, 128.7, 128.3, 119.3, 106.6, 104.0.

2-(3-bromophenyl)−6,7-dimethoxypyrido[2,3-d] pyrimidine (**3o**, Table 2). Eluent: Hexane/Ethyl acetate (10:1), Yellow solid (71%); IR

Table 3
Control Experiments.

| SI No | Variation from standard conditions[a] | Conversion[b] | |
		3a	4a
1	Standard conditions	99	n.d.
2	In the absence of **2a**	nd	39[c]
3	TEMPO(5 eq.)	90	Traces
4	12 h	75	4
5	NaO^tBu	Traces	Traces
6	In the presence of 18-crown-6	11	Traces

[a] Standard condition: 2-aminobenzyl alcohol (0.75 mmol), amide (0.5 mmol), base (1 mmol), solvent (2 ml), at 100 °C under Ar for 16 h. [b] Yield is determined by ^{1}H NMR spectroscopy using 1,4 dimethoxybenzene as the internal standard. [c] Yield refers to that of a pure product characterized by ^{1}H NMR.

(KBr) 1545, 1414, 1325, 1236, 1046, 805, 722 cm-1; ^{1}H NMR (500 MHz, CDCl$_3$) δ 9.13 (s, 1H), 8.65 (t, J = 1.7 Hz, 1H), 8.40 (dt, J = 7.8, 1.2 Hz, 1H), 7.52 (dq, J = 7.8, 1.0 Hz, 1H), 7.32–7.29 (m, 2H), 7.04 (s, 1H), 4.02 (s, 3H), 3.97 (s, 3H); ^{13}C NMR (125 MHz, CDCl$_3$) δ 157.4, 156.1, 155.4, 149.7, 147.6, 139.4, 131.9, 130.1, 129.0, 125.6, 121.9, 118.6, 105.8, 102.9, 55.5, 55.3.

6,7-dimethoxy-2-(3-methoxyphenyl) pyrido[2,3-d] pyrimidine (**3p**, Table 2). Eluent: Hexane/Ethyl acetate (5:1), Yellow solid (73%); IR (KBr) 1554, 1544, 1325, 1240, 1046, 799 cm^{-1}; ^{1}H NMR (500 MHz, CDCl$_3$) δ 9.12 (s, 1H), 8.07 (dd, J = 7.6, 1.1 Hz, 1H), 8.04 (q, J = 1.3 Hz, 1H), 7.34 (t, J = 7.9 Hz, 1H), 7.29 (s, 1H), 7.01 (s, 1H), 6.96 (d, J = 1.7 Hz, 1H), 4.00 (s, 3H), 3.95 (s, 3H), 3.86 (s, 3H); ^{13}C NMR (125 MHz, CDCl$_3$) δ 159.0, 158.7, 156.0, 155.2, 149.4, 147.6, 138.8, 128.5, 119.7, 118.4, 115.8, 111.6, 105.9, 102.9, 55.4, 55.2, 54.4.

Computational Details: DFT static calculations were performed with the Gaussian16 set of programs [96], using the BP86 functional of Becke and Perdew [97–99], including corrections due to dispersion through the Grimme's method (GD3 keyword in Gaussian16) [100,101]. The electronic configuration of the molecular systems was described with the double-ζ basis set with the polarization of Ahlrichs for main-group atoms (def2-SVP keyword in Gaussian) [102]. The geometry optimizations were performed without symmetry constraints, and analytical frequency calculations confirmed the character of the located stationary points. These frequencies were used to calculate unscaled zero-point energies (ZPEs) as well. Energies at 373.15 K were obtained by single-point calculations on the optimized geometries with the M06-D3 functional [103,104]. and the triple-ζ basis set def2-TZVPP and by estimating solvent effects with and estimation of solvent effects with the universal solvation model SMD of Cramer and Truhlar for amyl alcohol [105]. The reported Gibbs energies in this work include electronic energies obtained at the M06-D3/def2-TZVPP (smd)//BP86-D3/def2-SVP level of theory corrected with zero-point energies, thermal corrections and entropy effects computed with the BP86-D3/def2-SVP level.

3. Results and discussion

To optimize the reaction conditions, the reaction was studied with various reaction parameters such as reaction temperature, time, solvents, and the amount of base used, and the results are summarized in Table 1. Similarly, the ratio of the reactant was also standardized and reported in the supporting information. It was found that the maximum yield of the product was obtained with one equivalent of benzamide, 1.5 equivalents of 2-aminobenzyl alcohol, and two equivalents of KO^{t}Bu as a base in *t*-amyl alcohol at 100 °C for 16 h (entry 2, Table 1).

The solvent screening showed that toluene was slightly less effective than *t*-amyl alcohol and provided a relatively low yield (entries 1 and 2, Table 1). The conversion was dramatically influenced by polar aprotic solvents like DMF (entry 5, Table 1) and a more polar solvent like water (entry 6, Table 1). Time vs conversion plot (Fig. S2, SI) showed a minimum of 16 h reaction period was required for the completion of the reaction (entry 2, Table 1). Additionally, it had also been observed that to consume the limiting reagent (benzamide) completely, an excess (1.5 equivalents) of 2-aminobenzyl alcohol is required (Table 4, SI).

Furthermore, the reaction yield was significantly reduced when KO^{t}Bu was replaced by a weaker base (entries 9–12, Table 1). The reaction was not initiated with potassium carbonate as a base (entry 11, Table 1). Interestingly, during the optimization, we noticed that temperature plays a crucial role in this reaction. By decreasing the temperature to 80 °C, the conversion decreased drastically (entry 8,
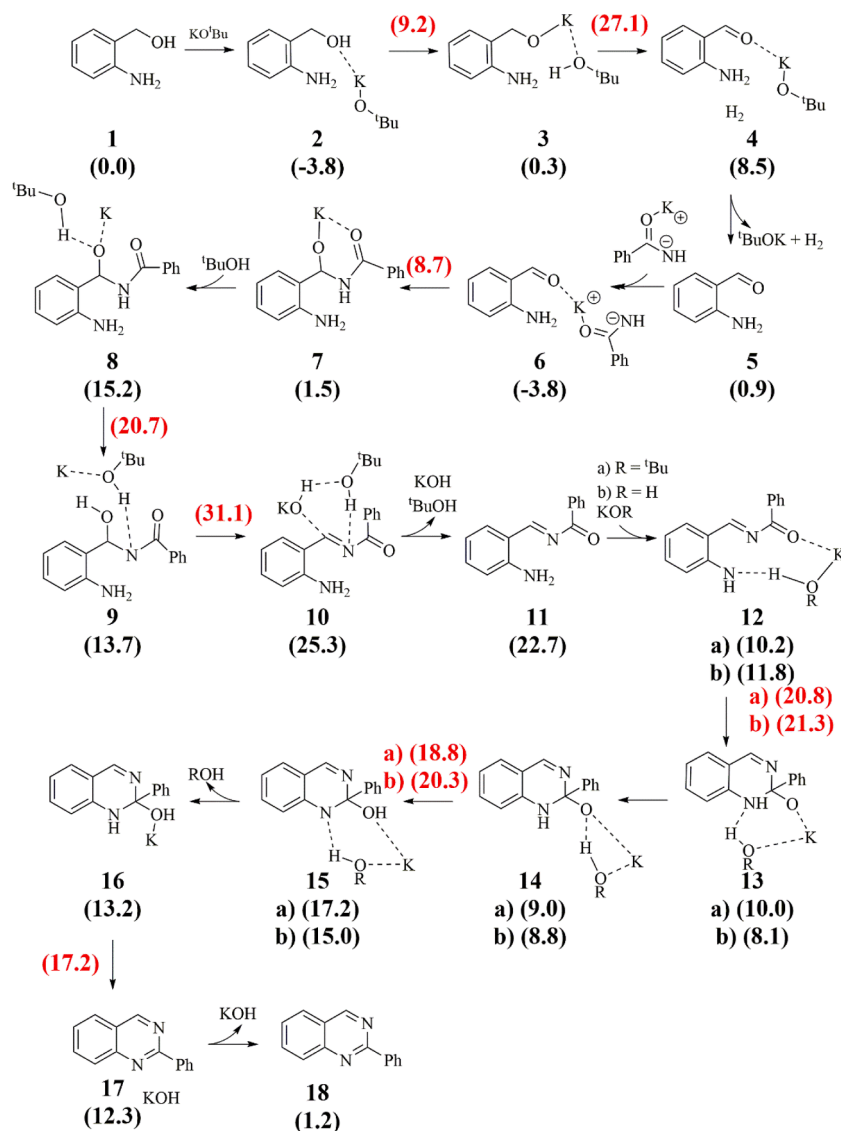
Fig. 2. Reaction mechanism leading to quinazoline derivatives starting from 2-aminobenzyl alcohol and aryl amide via an alcohol dehydrogenation strategy promoted by potassium tertiary butoxide (relative Gibbs energies in kcal/mol) at the M06-D3/def2-TZVPP(smd)//BP86-D3/def2-SVP level of theory.

Table 1). At room temperature, the response was futile (entry 7, Table 1). Several structurally varied substituted aryl and aliphatic amide underwent couplings with reaction intermediate generated in-situ from 2-aminobenzyl alcohol by this procedure to produce the corresponding quinazolines derivatives. The results are reported in Table 2.

Both aromatic and heterocyclic amides (**3k**, Table 2) participated efficiently in this reaction to form 2-substituted quinazolines (Table 2) irrespective of the electronic nature of the substituent present. However, ortho-substituted benzamides (**3c, 3d**, Table 2) react sluggishly, and even after 24 h of reaction, only 72% of corresponding products are isolated. The *meta*-substituted nitro benzamide also furnished a comparatively low yield (**3j**, Table 2). In general, the substituents at *m* and *p* position in aryl amides, e.g., 4-Me (**3a**, Table 2), 4-Cl (**3b**, Table 2), 3-Br (**3e**, Table 2), 4-Br (**3f**, Table 2), 4-OMe (3 h, Table 2) and 3-OMe (**3i**, Table 2), did not pose any difficulty to produce the corresponding quinazoline in high yields. Significantly, the reaction proceeded with aliphatic amide (**3l**, Table 2) without any interference. Moreover, substituted 2-aminobenzyl alcohol (**3n, 3o, 3p**, Table 2) and heteroaryl benzyl alcohol (3 m, Table 2) participated in the reaction effectively to furnish the corresponding product in good yield. This indicates the moderately good substrate scope for this reaction.

To understand the reaction mechanism and identify the reaction intermediate, several control experiments (Table 3) were performed at different time intervals and the results were critically analyzed. During the control reaction, in the absence of benzamide, we observed the formation of 39% of 2-aminobenzyladehyde as the product (entry 2, Table 3).

In another experiment, 4% of 2-aminobenzaldehyde was identified when the reaction was quenched at the intermediate stage (entry 4, Table 3), clearly indicating the formation of 2-amino benzaldehyde as an intermediate. Surprisingly, it has been observed that the NaO^{t}Bu was not effective in initiating the reaction (entry 5, Table 3). A similar trend was also noticed when we used NaOH (entry 12, Table 1) as a base when compared to KOH (entry 9, Table 1). we envisaged that the potassium ion plays a significant role in this reaction. To unravel this hypothesis, metal-ion trapping experiments with 18-crown-6 have been performed. In the presence of 18-crown-6, the progress of the reaction was affected remarkably (entry 6, Table 3), which undoubtedly indicates the crucial role of potassium ions in the reaction pathway. Anyway, it is not ensured if it acts catalytically. Furthermore, it has been observed that the presence of free radical quencher, TEMPO in excess, did not have much impact on the overall reaction progress (entry 3, Table 3). Therefore, the
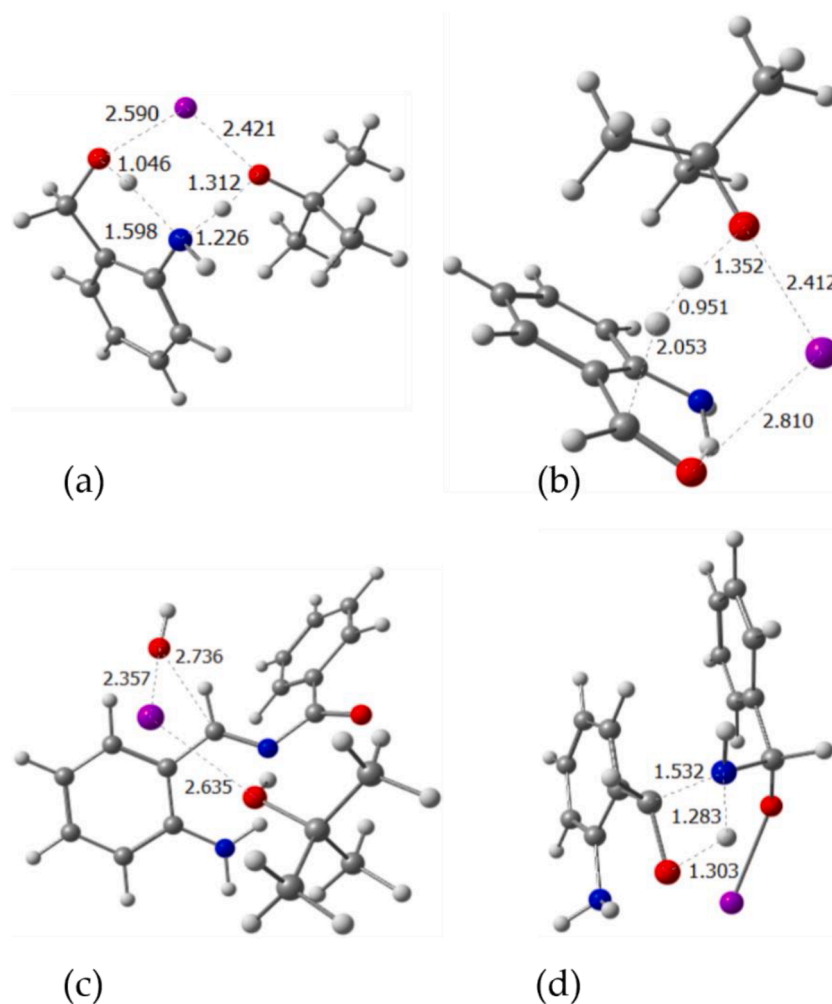
Fig. 3. 3D structures of the transition states (a) **TS 2→3**, (b) **TS 4→5**, (c) **TS 9→10** and (d) **TS 25→26** with a selection of distances in Å.

possibility of the free radical pathway has been discarded.

Berkessel *et al.* reported base-catalyzed hydrogenation of aromatic ketones and proposed a mechanism in which the reaction proceeds through a cyclic transition state involving carbonyl C=O, H—H, and O-K in KO^{t}Bu [106]. Since dehydrogenation is just the reverse of hydrogenation, a similar mechanism may also be operative for this potassium tertiary butoxide-promoted alcohol dehydrogenation. Based on the literature reports [77,106] and the results of the control experiments in Table 3, we believed that density functional theory (DFT) calculations could shed light on the reaction mechanism. Among the most plausible strategies, including alcohol dehydrogenation [83], hydrogenation without a metal catalyst [106], and borrowing hydrogen [71,107]. Fig. 2 includes the preferred mechanism calculated at the M06-D3/def2-TZVPP(smd)//BP86-D3/def2-SVP level of theory, following the metal-free transformation [108].

The mechanism in Fig. 2 begins with the proton transfer from the alcohol group of 2-aminobenzyl alcohol to KO^{t}Bu with the amino group that works as a proton shuttle. This step is kinetically feasible by overcoming an energy barrier of 13.0 kcal/mol through **TS 2→3** (see Fig. 3a). Therefore, from **3** the reaction proceeds through the six-membered ring transition state **TS 3→4** with an energy barrier of 26.8 kcal/mol such as in the dehydrogenation reported by Berkessel *et al.* (see Fig. 3b).

This step facilitates the formation of molecular hydrogen as well as the corresponding aldehyde **5**, which is nearly isoenergetic to the analogous initial alcohol **1**, simply being 0.9 kcal/mol higher in energy. At this point of the reaction, a unit of KO^{t}Bu removes one proton from the amide group of the other reagent. As a result, an amide anion

stabilized by potassium is formed and ^{t}BuOH is released into the solution. Thereafter, the anion reacts with the aldehyde **5**, to form an imine intermediate in several steps. As reported in the literature [109]. the imine formation is step-wise: first the carbinolamine formation, followed by the dehydration step. In our case study, the formation of the carbinolamine is not favored by the protic solvent, with the amyl alcohol acting as a proton shuttle that transfers a proton from the amine group to the carbonyl [110,111]. On the other hand, the potassium cation can activate the carbonyl groups and bring the reactants closer. In detail, here from **5** the reaction proceeds with the formation of complex **6** between aldehyde and the amide anion with a stabilization of 4.7 kcal/mol, considering that we omit the corrections of entropy and standard state of 1 M concentration in solution [112]. Subsequently, carbinolamine **7** is formed overcoming an energy barrier of 12.5 kcal/mol after the nucleophilic attack of the amide anion to the aldehyde carbonyl. Furthermore, the imine is formed not through dehydration, but by elimination of a KOH molecule. At the beginning, the rather unstable complex **8** with the protic solvent is formed and the remaining amino proton is transferred to the potassium alkoxide moieties forming a zwitterionic intermediate through **TS 8→9** overcoming an energy barrier of 5.5 kcal/mol in the subsequent step. Then, KOH is removed through **TS 9→10** ($\Delta G^{\ddagger}$ = 17.4 kcal/mol) and the imine **11** is formed after releasing KOH•••^{t}BuOH into the solution. The newly formed imine is deprotonated by KOH or KO^{t}Bu, forming complexes **12**. Then, the deprotonated amino group reacts with the aldehyde moiety forming a six-membered ring of potassium amino alkoxide **13** through **TS 12→13**, overcoming energy barriers of 10.6 and 9.5 kcal/mol with R = ^{t}Bu and
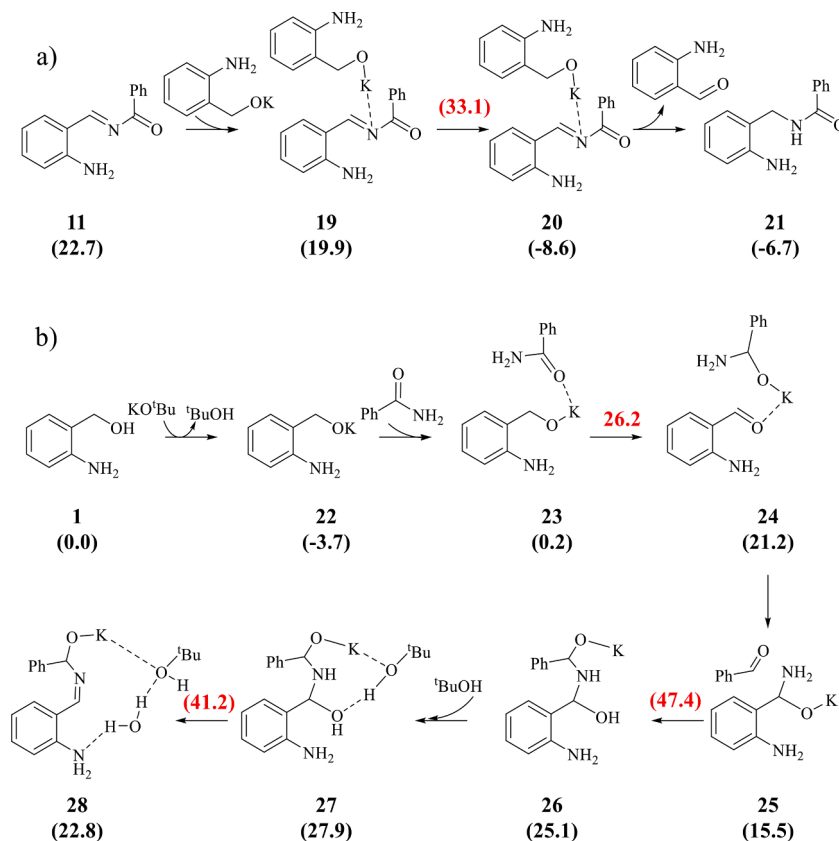
Fig. 4. Alternative mechanisms/steps are leading to quinazoline derivatives starting from 2-aminobenzyl alcohol and aryl amide by potassium tertiary butoxide (relative Gibbs energies in kcal/mol) at the M06-D3/def2-TZVPP(smd)//BP86-D3/def2-SVP level of theory.

H, respectively. Next, either H_2O or ^tBuOH, activated by potassium cation, takes the remaining amino proton with a slightly less kinetically transition state and transfers it to the potassium alkoxide moiety forming the zwitterionic intermediates **15**, thus being just proton shuttles. H_2O and ^tBuOH are then released into the solution to form intermediate **16**. Finally, the quinazoline product **18** is formed by releasing a KOH molecule, overcoming an energy barrier of only 5.0 kcal/mol corresponding to **TS 16→17**. Overall, the step defined by **TS 9→10** results to be the rate determining step [113], actually the rate-determining state (rds) [114] of the whole reaction mechanism, with an overall kinetic cost of 34.9 kcal/mol [115–117]. However, it is also necessary to consider above all the other determining step, which is **TS 3→4**, the reason derives from seeing that if we replace KO^{t}Bu with NaO^{t}Bu as a reagent, the rds described as **TS 16→17** remains almost isoenergetic, and even being 0.4 kcal/mol lower, while the step defined by **TS 9→10** does get significantly worse by 2.2 kcal/mol. To give more reliability to this trend, the **TS 16→17** was also studied. Although it would not be decisive for anything, it is also seen how its kinetic cost increases by 2.6 kcal/mol with the sodium ion. This leads us to conclude that sodium as a countercation of the base has a worse behavior than potassium. Moreover, it gives us feedback by making us see that the rds would not be **TS 9→10** but **TS 3→4**, thus being a kinetic cost of 30.9 kcal/mol, also more in agreement with the experimental temperature of 100 °C. The reason why the **TS 9→10** barrier is overestimated is that even though it was attempted, more than one ^tBuOH molecule would have to be involved.

An alternative mechanisms has also been proposed in Fig. 4 starting with imine **11** where one molecule of 2-aminobenzyl alcohol hydrogenated the imine group similarly to the pyridine-mediated alcohol oxidation reported by Namitharan and coworkers [107]. The 2-aminobenzyl alcohol is deprotonated to form the corresponding potassium alkoxide. Next, the potassium alkoxide forms complex **19** with imine **11** required to overcome **TS 19→20** with an overall kinetic cost of 36.9

kcal/mol, which discards this alternative mechanism. On the other hand, another mechanism starts with the formation of the potassium 2-aminobenzyl alkoxide **22**, with a favorable energy gain of −3.7 kcal/mol. The alkoxide then forms the adduct **23** with the amide. Next, overcoming an energy barrier of 26.0 kcal/mol there is the H-transfer that leads to intermediate **24**, with the fundamental role of the potassium cation to stabilize the negative charge of any of the oxygen atoms involved. Through the rotational movement of the K-O-C—N dihedral angle, complex **24** isomerizes into complex **25** to facilitate the proton transfer from the amino group to the carbonyl. However, although the aldehyde is activated by potassium, the condensation of aldehyde with the amine group results to be expensive in terms of kinetics ($\Delta G^{\ddagger} = 31.9$ kcal/mol) and it leads to the formation of species **26** (see Fig. 3d). The next step, the dehydration step [37,38,118], results to be expensive too even if assisted by a solvent molecule [119–121]. First, intermediate **27** is formed and, then the remaining amino proton is transferred through **TS 27→28** ($\Delta G^{\ddagger} = 13.3$ kcal/mol) to the hydroxyl group meanwhile the latter one is acting as a leaving group. Anyway, the latter steps lead to an overall kinetic cost of up to 51.2 kcal/mol. Since both of the latter mechanisms discussed are higher in energy with respect to the one displayed in Fig. 2, they were discarded.

4. Conclusions

In conclusion, we have developed a methodology for the synthesis of substituted quinazolines under transition metal-free reaction conditions, and omitting oxidations working under argon atmosphere [122]. Controlled experiments were carried out to elucidate the reaction mechanism. The role of K^+ ions was established by trapping with 18-crown-6-ether. The DFT calculations not only unveiled the reaction mechanism but also justify the reaction conditions, laying the groundwork for improving them even further by describing the most kinetically

demanding steps. The present method offers operational simplicity and general applicability to synthesize a wide range of 2-substituted quinazolines derivatives (including alkyl, aryl, and heterocyclic), with good to excellent yields of products. To the best of our knowledge, we are unaware of any report for quinazoline synthesis starting from 2-amino-benzyl alcohol and amides as substrates without using a transition metal as a catalyst.

Author contributions

All authors have read and agreed to the published version of the manuscript. Hima P and Vageesh M run all experiments. Michele Tomasini performed all the calculations. Hima P, Vageesh M and Michele Tomasini performed the visualization and wrote the original draft. Albert Poater and Raju Dey performed the analysis, supervision, review and editing of the text.

CRediT authorship contribution statement

Hima P: Investigation, Data curation. **Vageesh M:** Investigation, Data curation. **Michele Tomasini:** Investigation, Data curation, Funding acquisition. **Albert Poater:** Investigation, Data curation, Funding acquisition. **Raju Dey:** Supervision, Conceptualization, Funding acquisition, Writing – review & editing.

Declaration of Competing Interest

The authors declare that they have no known competing financial interests or personal relationships that could have appeared to influence the work reported in this paper.

Data availability

A summary is collected in the supporting information file and then more details are available upon request.

Acknowledgments

Supplementary materials

Supplementary material associated with this article can be found, in the online version, at doi:10.1016/j.mcat.2023.113110.

References

[1] A. Al-Mulla, A. Review, Biological importance of heterocyclic compounds, Der Pharma Chem 9 (2017) 141–147.

[2] X.F. Shang, S.L. Morris-Natschke, Y.-.Q. Liu, X.-.S. Guo, X.-.S. Xu, M. Goto, J.-. C. Li, G.-.Z. Yang, K.-.H. Lee, Biologically active quinoline and quinazoline alkaloids part I, Med. Res. Rev. 38 (2018) 775–828.

[3] M.M. Ghorab, Z.H. Ismail, A.A. Radwan, M. Abdalla, Synthesis and pharmacophore modeling of novel quinazolines bearing a biologically active sulfonamide moiety, Acta Pharm 63 (2013) 1–18.

[4] A.A. Al-Amiery, A.A.H. Kadhum, M. Shamel, M. Satar, Y. Khalid, A.B. Mohamad, Antioxidant and antimicrobial activities of novel quinazolinones, Med. Chem. Res. 23 (2014) 236–242.

[5] R.S. Giri, H.M. Thaker, T. Giordano, J. Williams, D. Rogers, V. Sudersanam, K. K. Vasu, Design, synthesis and characterization of novel 2-(2,4-disubstituted-thiazole-5-yl)-3-aryl-3H-quinazoline-4-one derivatives as inhibitors of NF-κB and AP-1 mediated transcription activation and as potential anti-inflammatory agents, Eur. J. Med. Chem. 44 (2009) 2184–2189.

[6] A. Chugh, A. Kumar, A. Verma, S. Kumar, P. Kumar, A review of antimalarial activity of two or three nitrogen atoms containing heterocyclic compounds, Med. Chem. Res. 29 (2020) 1723–17500.

[7] M.J. Deetz, J.P. Malerich, A.M. Beatty, B.D. Smith, One-step synthesis of 4(3H) quinazolinones, Tetrahedron Lett. 42 (2001) 1851–1854.

[8] A. Mermer, T. Keles, Y. Sirin, Recent studies of nitrogen containing heterocyclic compounds as novel antiviral agents: a review, Bioorg. Chem. 114 (2021), 105076.

[9] J. Kunes, J. Bazant, M. Pour, K. Waisser, M. Slosárek, J. Janota, Quinazoline derivatives with antitubercular activity, Farmaco 55 (2000) 725–729.

[10] E. Honkanen, A. Pippuri, P. Kairisalo, P. Nore, H. Karppanen, I. Paakkari, Synthesis and antihypertensive activity of some new quinazoline derivatives, J. Med. Chem. 26 (1983) 1433–1438.

[11] S. Sasmal, D. Balasubrahmanyam, H.R.K. Reddy, G. Balaji, G. Srinivas, S. Cheera, C. Abbineni, P.K. Sasmal, I. Khanna, V.J. Sebastian, V.P. Jadhav, M.P. Singh, R. Talwar, J. Suresh, D. Shashikumar, K.H. Reddy, V. Sihorkar, T.M. Frimurer, Ø. Rist, L. Elster, T. Högberg, Design and optimization of quinazoline derivatives as melanin concentrating hormone receptor 1 (MCHR1) antagonists: part 2, Bioorg. Med. Chem. Lett. 22 (2012) 3163–3167.

[12] M. Alvarado, M. Barceló, L. Carro, C.F. Masaguer, E. Raviña, Synthesis and biological evaluation of new quinazoline and cinnoline derivatives as potential atypical antipsychotics, Chem. Biodivers. 1 (2006) 106–117.

[13] R. Karan, P. Agarwal, M. Sinha, N. Mahato, Recent advances on quinazoline derivatives: a potential bioactive scaffold in medicinal chemistry, ChemEngineering 5 (2021) 73.

[14] S. Liu, F. Liu, X. Yu, G. Ding, P. Xu, J. Cao, Y. Jiang, The 3D-QSAR analysis of 4 (3H)-quinazolinone derivatives with dithiocarbamate side chains on thymidylate synthase, Bioorg. Med. Chem. 14 (2006) 1425–1430.

[15] J. Guiles, X. Sun, I.A. Critchley, U. Ochsner, M. Tregay, K. Stone, J. Bertino, L. Green, R. Sabin, F. Dean, H. Garry Dallmann, C.S. McHenry, N. Janjic, Quinazolin-2-ylamino-quinazolin-4-ols as novel non-nucleoside inhibitors of bacterial DNA polymerase III, Bioorg. Med. Chem. Lett. 19 (2009) 800–802.

[16] M.T. Conconi, G. Marzaro, L. Urbani, I. Zanusso, R. Di Liddo, I. Castagliuolo, P. Brun, F. Tonus, A. Ferrarese, A. Guiotto, A. Chilin, Quinazoline-based multi-tyrosine kinase inhibitors: synthesis, modeling, antitumor and antiangiogenic properties, Eur. J. Med. Chem. 67 (2013) 373–383.

[17] N. Kyprianou, Doxazosin and terazosin suppress prostate growth by inducing apoptosis: clinical significance, J. Urol. 169 (2003) 1520–1525.

[18] D. Wang, F. Gao, Quinazoline derivatives: synthesis and bioactivities, Chem. Cent. J 7 (2013) 95.

[19] J.J. Vanden Eynde, J. Godin, A. Mayence, A. Maquestiau, E. Anders, A New and convenient method for the preparation of 2-substituted quinazolines, Synthesis (Mass) (1993) 867–869.

[20] A.R. Tiwari, B.M. Bhanage, Chemoselective cleavage of C(CO)−C bond: molecular iodine-catalyzed synthesis of quinazolines through sp^3 C− H bond functionalization of aryl methyl ketones, Asian J. Org. Chem. 6 (2017) 831–836.

[21] C.U. Maheswari, G.S. Kumar, M. Venkateshwar, R.A. Kumar, M.L. Kantam, K. R. Reddy, Highly efficient one-pot synthesis of 2-substituted quinazolines and 4H-benzo[d][1,3]oxazines via cross dehydrogenative coupling using sodium hypochlorite, Adv. Synth. Catal. 352 (2010) 341–346.

[22] V.L. Truong, M. Morrow, Mild and efficient ligand-free copper-catalyzed condensation for the synthesis of quinazolines, Tetrahedron Lett. 51 (2010) 758–760.

[23] C. Xu, F.C. Jia, Z.W. Zhou, S.J. Zheng, H. Li, A.X. Wu, Copper-catalyzed multicomponent domino reaction of 2-bromoaldehydes, benzylamines, and sodium azide for the assembly of quinazoline derivatives, J. Org. Chem. 81 (2016) 3000–3006.

[24] S. Yao, K. Zhou, J. Wang, H. Cao, L. Yu, J. Wu, P. Qiu, Q. Xu, Synthesis of 2-substituted quinazolines by CsOH-mediated direct aerobic oxidative cyclocondensation of 2-aminoarylmethanols with nitriles in air, Green Chem 19 (2017) 2945–2951.

[25] T. Chatterjee, D.I. Kim, E.J. Cho, Base-promoted synthesis of 2-aryl quinazolines from 2-aminobenzylamines in water, J. Org. Chem. 83 (2018) 7423–7430.

[26] C. Huang, Y. Fu, H. Fu, Y. Jiang, Y. Zhao, Highly efficient copper-catalyzed cascade synthesis of quinazoline and quinazolinone derivatives, Chem. Commun. (2008) 6333–6335.

[27] Z.H. Zhang, X.N. Zhang, L.P. Mo, Y.X. Li, F.P. Ma, Catalyst-free synthesis of quinazoline derivatives using low melting sugar–urea–salt mixture as a solvent, Green Chem 14 (2012) 1502–1506.

[28] V.L. Truong, M. Morrow, Mild and efficient ligand-free copper-catalyzed condensation for the synthesis of quinazolines, Tetrahedron Lett 51 (2010) 758–760.

[29] Y. Peng, Y. Zeng, G. Qiu, L. Cai, V.W. Pike, A convenient one-pot procedure for the synthesis of 2-aryl quinazolines using active MnO$_2$ as oxidant, J. Heterocycl. Chem. 47 (2010) 1240–1245.

[30] Z. Chen, J. Chen, M. Liu, J. Ding, W. Gao, X. Huang, H. Wu, Unexpected copper-catalyzed cascade synthesis of quinazoline derivatives, J. Org. Chem. 78 (2013) 11342–11348.

[31] C. Gunanathan, D. Milstein, Applications of acceptorless dehydrogenation and related transformations in chemical synthesis, Science 341 (2013), 1229712.

[32] K. Sun, H. Shan, G.-P. Lu, C. Cai, M. Beller, Synthesis of N-heterocycles via oxidant-free dehydrocyclization of alcohols using heterogeneous catalysts, Angew. Chem. Int. Ed. 60 (2021) 25188–25202.

[33] J.C. Borghs, V. Zubar, L.M. Azofra, J. Sklyaruk, M. Rueping, Manganese-catalyzed regioselective dehydrogenative C-versus N-alkylation enabled by a solvent switch: experiment and computation, Org. Lett. 22 (2020) 4222–4227.

[34] L.M. Azofra, A. Poater, Diastereoselective Diazenyl formation: the Key For Manganese-Catalysed Alcohol Conversion Into (E)-alkenes, 48, Dalton Trans, 2019, pp. 14122–14127.

[35] J. Masdemont, J.A. Luque-Urrutia, M. Gimferrer, D. Milstein, A. Poater, Mechanism of coupling of alcohols and amines to generate aldimines and H_2 by a pincer manganese catalyst, ACS Catal. 9 (2019) 1662–1669.

[36] J.A. Luque-Urrutia, T. Pèlachs, M. Solà, A. Poater, Double-carrousel mechanism for Mn-catalyzed dehydrogenative amide synthesis from alcohols and amines, ACS Catal. 11 (2021) 6155–6161.

[37] J.A. Luque-Urrutia, M. Solà, D. Milstein, A. Poater, Mechanism of the manganese-pincer catalyzed acceptorless dehydrogenative coupling of nitriles and alcohols, J. Am. Chem. Soc. 141 (2019) 2398–2403.

[38] A. Cicolella, M.C. D'Alterio, J. Duran, S. Simon, G. Talarico, A. Poater, Combining both acceptorless dehydrogenation and borrowing hydrogen mechanisms in one system as described by DFT calculations, Adv. Theory Simul. 5 (2022) 2100566.

[39] S. Parua, R. Sikari, S. Sinha, G. Chakraborty, R. Mondal, N.D. Paul, Accessing polysubstituted quinazolines via nickel catalyzed acceptorless dehydrogenative coupling, J. Org. Chem. 83 (2018) 11154–11166.

[40] A. Mondal, M.K. Sahoo, M. Subaramanian, E. Balaraman, Manganese(I)-catalyzed sustainable synthesis of quinoxaline and quinazoline derivatives with the liberation of dihydrogen, J. Org. Chem. 85 (2020) 7181–7191.

[41] K. Das, A. Mondal, D. Pal, D. Srimani, Sustainable synthesis of quinazoline and 2-aminoquinoline via dehydrogenative coupling of 2-aminobenzyl alcohol and nitrile catalyzed by phosphine-free manganese pincer complex, Org. Lett. 21 (2019) 3223–3227.

[42] G. Chakraborty, R. Sikari, S. Das, R. Mondal, S. Sinha, S. Banerjee, N.D. Paul, Dehydrogenative synthesis of quinolines, 2-aminoquinolines, and quinazolines using singlet diradical Ni(II)-catalysts, J. Org. Chem. 84 (2019) 2626–2641.

[43] X.-M. Wan, Z.L. Liu, W.-Q. Liu, X.-N. Cao, X. Zhu, X.-M. Zhao, B. Song, X.-Q. Hao, G. Liu, NNN pincer Ru(II)-catalyzed dehydrogenative coupling of 2-aminoarylmethanols with nitriles for the construction of quinazolines, Tetrahedron 75 (2019) 2697–2705.

[44] S.-Q. Zhang, B. Guo, D.J. Young, Z. Xu, H.-X. Li, Efficient synthesis of quinazolines by the iron-catalyzed acceptorless dehydrogenative coupling of (2-aminophenyl)methanols and benzamides, Tetrahedron 78 (2021) 131825.

[45] S. Elangovan, J. Neumann, J.B. Sortais, B. Junge, C. Darcel, M. Beller, Efficient and selective N-alkylation of amines with alcohols catalysed by manganese pincer complexes, Nat. Commun. 7 (2016) 12641.

[46] S. Waiba, B. Maji, Manganese catalyzed acceptorless dehydrogenative coupling reactions, ChemCatChem 12 (2019) 1891–1902.

[47] A. Mukherjee, A. Nerush, G. Leitus, L.J.W. Shimon, Y.B. David, N.A.E. Jalapa, D. Milstein, Manganese-catalyzed environmentally benign dehydrogenative coupling of alcohols and amines to form aldimines and H_2: a catalytic and mechanistic study, J. Am. Chem. Soc. 138 (2016) 4298–4301.

[48] M. Mastalir, M. Glatz, E. Pittenauer, G. Allmaier, K. Kirchner, Sustainable synthesis of quinolines and pyrimidines catalyzed by manganese PNP pincer complexes, J. Am. Chem. Soc. 138 (2016) 15543–15546.

[49] N. Deibl, R. Kempe, Manganese-catalyzed multicomponent synthesis of pyrimidines from alcohols and amidines, Angew. Chem. Int. Ed. 56 (2017) 1663–1666.

[50] E. Balaraman, A. Nandakumar, G. Jaiswalab, M.K. Sahoo, Iron-catalyzed dehydrogenation reactions and their applications in sustainable energy and catalysis, Catal. Sci. Technol. 7 (2017) 3177–3195.

[51] G. Jaiswal, V.G. Landge, D. Jagadeesan, E. Balaraman, Iron-based nanocatalyst for the acceptorless dehydrogenation reactions, Nat. Commun. 8 (2017) 2147.

[52] V. Arun, K. Mahanty, S. De Sarkar, Nickel-catalyzed dehydrogenative couplings, ChemCatChem 11 (2019) 2243–2259.

[53] S. Das, D. Maiti, S. De Sarkar, Synthesis of polysubstituted quinolines from α-2-aminoaryl alcohols via nickel-catalyzed dehydrogenative coupling, J. Org. Chem. 83 (2018) 2309–2316.

[54] S. Chakraborty, P.E. Piszel, W.W. Brennessel, W.D. Jones, A single nickel catalyst for the acceptorless dehydrogenation of alcohols and hydrogenation of carbonyl compounds, Organometallics 34 (2015) 5203–5206.

[55] I. Borthakur, A. Sau, S. Kundu, Cobalt-catalyzed dehydrogenative functionalization of alcohols: progress and future prospect, Coord. Chem. Rev. 451 (2022), 214257.

[56] K.-i. Shimizu, K. Kon, M. Seto, K. Shimura, H. Yamazaki, J.N. Kondo, Heterogeneous cobalt catalysts for the acceptorless dehydrogenation of alcohols, Green Chem. 15 (2013) 418–424.

[57] K. Junge, V. Papa, M. Beller, Cobalt–pincer complexes in catalysis, Chem. Eur. J. 25 (2019) 122–143.

[58] D.R. Pradhan, S. Pattanaik, J. Kishore, C. Gunanathan, Cobalt-catalyzed acceptorless dehydrogenation of alcohols to carboxylate salts and hydrogen, Org. Lett. 22 (2020) 1852–1857.

[59] G. Zhang, S.K. Hanson, Cobalt-catalyzed acceptorless alcohol dehydrogenation: synthesis of imines from alcohols and amines, Org. Lett. 15 (2013) 650–653.

[60] J. Choi, A.H.R. MacArthur, M. Brookhart, A.S. Goldman, Dehydrogenation and related reactions catalyzed by iridium pincer complexes, Chem. Rev. 111 (2011) 1761–1779.

[61] K. Chakrabarti, M. Maji, S. Kundu, Cooperative iridium complex-catalyzed synthesis of quinoxalines, benzimidazoles and quinazolines in water, Green Chem. 21 (2019) 1999–2004.

[62] K. Wada, H. Yu, Q. Feng, Titania-supported iridium catalysts for dehydrogenative synthesis of benzimidazoles, Chin. Chem. Lett. 31 (2020) 605–608.

[63] M. Maji, K. Chakrabarti, D. Panja, S. Kundu, Sustainable synthesis of N-heterocycles in water using alcohols following the double dehydrogenation strategy, J. Catal. 373 (2019) 93–102.

[64] T. Mitsudome, Y. Mikami, H. Funai, T. Mizugaki, K. Jitsukawa, K. Kaneda, Oxidant-free alcohol dehydrogenation using a reusable hydrotalcite-supported silver nanoparticle catalyst, Angew. Chem. Int. Ed. 47 (2008) 138–141.

[65] X. Wang, C. Wang, Y. Liu, J. Xiao, Acceptorless dehydrogenation and aerobic oxidation of alcohols with a reusable binuclear rhodium(II) catalyst in water, Green Chem 18 (2016) 4605–4610.

[66] B. Gnanaprakasam, J. Zhang, D. Milstein, Direct synthesis of imines from alcohols and amines with liberation of H_2, Angew. Chem. Int. Ed. 49 (2010) 1468–1471.

[67] M. Maji, K. Chakrabarti, B. Paul, B.C. Roy, S. Kundu, Ruthenium(II)-NNN-pincer-complex-catalyzed reactions between various alcohols and amines for sustainable C—N and C—C bond formation, Adv. Synth. Catal. 360 (2018) 722–729.

[68] G. Chelucci, S. Baldino, W. Baratta, Recent advances in osmium-catalyzed hydrogenation and dehydrogenation reactions, Acc. Chem. Res. 48 (2015) 363–379.

[69] S.S. Poly, S.M.A. Hakim Siddiki, A.S. Touchy, K.W. Ting, T. Toyao, Z. Maeno, Y. Kanda, K.-i. Shimizu, Acceptorless dehydrogenative synthesis of pyrimidines from alcohols and amidines catalyzed by supported platinum nanoparticles, ACS Catal. 8 (2018) 11330–11341.

[70] M. Trincado, J. Bösken, H. Grützmacher, Homogeneously catalyzed acceptorless dehydrogenation of alcohols: a progress report, Coord. Chem. Rev. 443 (2021), 213967.

[71] T. Irrgang, R. Kempe, 3d-metal catalyzed N- and C-alkylation reactions via borrowing hydrogen or hydrogen autotransfer, Chem. Rev. 119 (2019) 2524–2549.

[72] K.S. Egorova, V.P. Ananikov, Toxicity of metal compounds: knowledge and myths, Organometallics 36 (2017) 4071–4090.

[73] B.C. Ranu, A. Saha, R. Dey, Using more environmentally friendly solvents and benign catalysts in performing conventional organic reactions, Curr. Opin. Drug. Discov. Devel. 13 (2010) 658–668.

[74] A. Batra, P. Singh, K.N. Singh, Latest advancements in transition-metal-free carbon-heteroatom bond formation reactions via cross- dehydrogenative coupling, Asian J. Org. Chem. 10 (2021) 1024–1049.

[75] K. Motokura, R. Sato, N. Ozawa, Y. Manaka, Transition-metal-free reaction sequence on solid base: one-pot synthesis of quinoline derivatives catalyzed by Mg-Al hydrotalcite, Mol. Catal. 528 (2022), 112419.

[76] R. Dey, B.C. Ranu, A convenient and efficient protocol for the synthesis of 4(1H)-cinnolones,1,4-dihydrocinnolines, and cinnolines in aqueous medium: application for detection of nitrite ions, Tetrahedron 67 (2011) 8918–8924.

[77] L.J. Allen, R.H. Crabtree, Green alcohol couplings without transition metal catalysts: base-mediated β-alkylation of alcohols in aerobic conditions, Green Chem. 12 (2010) 1362–1364.

[78] Y. Kita, M. Kuwabara, K. Kamata, M. Hara, Heterogeneous low-valent mn catalysts for α-alkylation of ketones with alcohols through borrowing hydrogen methodology, ACS Catal. 12 (2022) 11767–11775.

[79] J. Liu, C. Li, H. Niu, C. Liang, Role of metal (Pt)-support (MgO) interactions in base-free glucose dehydrogenation, Catal. Sci. Technol. 12 (2022) 6849–6855.

[80] M. Subaramanian, G. Sivakumar, E. Balaraman, First-row transition-metal catalyzed acceptorless dehydrogenation and related reactions: a personal account, Chem. Rec. 21 (2021) 3839–3871.

[81] S. Nishimura, A. Takagaki, K. Ebitani, Characterization, synthesis and catalysis of hydrotalcite-related materials for highly efficient materials transformations, Green Chem. 15 (2013) 2026–2042.

[82] A.A. Toutov, W.-.B. Liu, K.N. Betz, A. Fedorov, B.M. Stoltz, R.H. Grubbs, Silylation of C–H bonds in aromatic heterocycles by an Earth-abundant metal catalyst, Nature 518 (2015) 80–84.

[83] T. Liu, K. Wu, L. Wang, Z. Yu, Potassium tert-butoxide-promoted acceptorless dehydrogenation of N-heterocycles, Adv. Synth. Catal. 361 (2019) 3958–3964.

[84] G. Li, M. Li, Z. Xia, C. Tan, W. Deng, C. Fang, Direct synthesis of amides from benzonitriles and benzylic alcohols via a KO t-Bu-mediated MPV-type hydrogen transfer process, J. Org. Chem. 87 (2022) 8884–8891.

[85] R. Gujjarappa, S.K. Maity, C.K. Hazra, N. Vodnala, S. Dhiman, A. Kumar, U. Beifuss, C.C. Malakar, Divergent synthesis of quinazolines using organocatalytic domino strategies under aerobic conditions, Eur. J. Org. Chem. (2018) 4628–4638.

[86] K. Gopalaiah, A. Saini, A. Devi, Iron-catalyzed cascade reaction of 2-aminobenzyl alcohols with benzylamines: synthesis of quinazolines by trapping of ammonia, Org. Biomol. Chem. 15 (2017) 5781–5789.

[87] J. Ma, Y. Wan, C. Hong, M. Li, X. Hu, W. Mo, B. Hu, N. Sun, L. Jin, Z. Shen, ABNO-catalyzed aerobic oxidative synthesis of 2-substituted 4H-3,1-benzoxazines and quinazolines, Eur. J. Org. Chem. (2017) 3335–3342.

[88] M. Martos, I.M. Pastor, Iron-based imidazolium salt as dual Lewis acid and redox catalyst for the aerobic synthesis of quinazolines, Eur. J. Org. Chem. 2022 (2022), e202200839.

[89] R. Gujjarappa, N. Vodnala, V. Ganga Reddy, C.C. Malakar, Niacin as a potent organocatalyst towards the synthesis of quinazolines using nitriles as C–N source, Eur. J. Org. Chem. 2020 (2020) 803–814.

[90] E. Eidi, M.Z. Kassaee, Z. Nasresfahani, P.T. Cummings, Synthesis of quinazolines over recyclable $Fe_3O_4@SiO_2$-$PrNH_2$-Fe^{3+} nanoparticles: a green, efficient, and solvent-free protocol, Appl. Organomet. Chem. 32 (2018) e4573.

[91] S. Ferrini, F. Ponticelli, M. Taddei, Convenient synthetic approach to 2,4-disubstituted quinazolines, Org. Lett. 9 (2007) 69–72.

[92] Y. Yan, Y. Zhang, Chengtao Feng, Z. Zha, Z. Wang, Selective iodine-catalyzed intermolecular oxidative amination of $C(sp^3)$-H bonds with ortho-carbonyl-substituted anilines to give quinazolines, Angew. Chem. Int. Ed. 51 (2012) 8077–8081.

[93] U. Pratim Saikia, G. Borah, P. Pahari, Lewis-acid-catalysed activation of nitriles: a microwave-assisted solvent-free synthesis of 2,4-disubstituted quinazolines and 1,3-diazaspiro[5.5]undec-1-enes, Eur. J. Org. Chem. (2018) 1211–1217.

[94] Y. Yan, Y. Xu, B. Niu, H. Xie, Y. Liu, I2-catalyzed aerobic oxidative $C(sp^3)$–H Amination/C–N cleavage of tertiary amine: synthesis of quinazolines and quinazolinones, J. Org. Chem. 80 (2015) 5581–5587.

[95] R. Wang, S. Liu, L. Li, A. Song, S. Yu, S. Zhuo, L.-.B. Xing, Metal-free catalyst for the visible-light-induced photocatalytic synthesis of quinazolinones, Mol. Catal. 509 (2021) 111668.

[96] M.J. Frisch, G.W. Trucks, H.B. Schlegel, G.E. Scuseria, M.A. Robb, J. R. Cheeseman, G. Scalmani, V. Barone, G.A. Petersson, H. Nakatsuji, X. Li, M. Caricato, A.V. Marenich, J Bloino, B.G. Janesko, R. Gomperts, B. Mennucci, H. P. Hratchian, J.V. Ortiz, A.F. Izmaylov, J.L. Sonnenberg, D. Williams-Young, F. Ding, F. Lipparini, F. Egidi, J. Goings, B. Peng, A. Petrone, T. Henderson, D. Ranasinghe, V.G. Zakrzewski, J. Gao, N. Rega, G. Zheng, W. Liang, M. Hada, M. Ehara, K. Toyota, R. Fukuda, J. Hasegawa, M. Ishida, T. Nakajima, Y. Honda, O. Kitao, H. Nakai, T. Vreven, K. Throssell, J.A. Montgomery Jr., J.E. Peralta, F. Ogliaro, M.J. Bearpark, J.J. Heyd, E.N. Brothers, K.N. Kudin, V.N. Staroverov, T.A. Keith, R. Kobayashi, J. Normand, K. Raghavachari, A.P. Rendell, J.C. Burant, S.S. Iyengar, J. Tomasi, M. Cossi, J.M. Millam, M. Klene, C. Adamo, R. Cammi, J. W. Ochterski, R.L. Martin, K. Morokuma, O. Farkas, J.B. Foresman, D.J. Fox, Gaussian 16, Revision C.01, Gaussian, Inc., Wallingford CT, 2016.

[97] J.P. Perdew, Density-functional approximation for the correlation energy of the inhomogeneous electron gas, Phys. Rev. B 33 (1986) 8822–8824.

[98] A.D. Becke, Density-functional exchange-energy approximation with correct asymptotic behavior, Phys. Rev. A 38 (1988) 3098–3100.

[99] J.P. Perdew, Erratum: density-functional approximation for the correlation energy of the inhomogeneous electron gas, Phys. Rev. B 34 (1986) 7406.

[100] S. Grimme, J. Antony, S. Ehrlich, H. Krieg, A consistent and accurate ab initio parametrization of density functional dispersion correction (DFT-D) for the 94 elements H-Pu, J. Chem. Phys. 132 (2010), 154104.

[101] S. Grimme, Semiempirical hybrid density functional with perturbative second-order correlation, J. Chem. Phys. 124 (2006), 034108.

[102] F. Weigend, R. Ahlrichs, Balanced basis sets of split valence, triple zeta valence and quadruple zeta valence quality for H to Rn: design and assessment of accuracy, Phys. Chem. Chem. Phys. 7 (2005) 3297–3305.

[103] Y. Zhao, D.G. Truhlar, The M06 suite of density functionals for main group thermochemistry, thermochemical kinetics, noncovalent interactions, excited states, and transition elements: two new functionals and systematic testing of four M06-class functionals and 12 other functionals, Theor. Chem. Acc. 120 (2008) 215–241.

[104] Y. Zhao, D.G. Truhlar, A new local density functional for main-group thermochemistry, transition metal bonding, thermochemical kinetics, and noncovalent interactions, J. Chem. Phys. 125 (2006), 194101.

[105] A.V. Marenich, C.J. Cramer, D.G. Truhlar, Universal solvation model based on solute electron density and a continuum model of the solvent defined by the bulk dielectric constant and atomic surface tensions, J. Phys. Chem. B 113 (2009) 6378–6396.

[106] A. Berkessel, T.J.S. Schubert, T.N. Muller, Hydrogenation without a transition-metal catalyst: on the mechanism of the base-catalyzed hydrogenation of ketones, J. Am. Chem. Soc. 124 (2002) 8693–8698.

[107] R. Pothikumar, V.T. Bhat, K. Namitharan, Pyridine mediated transition-metal-free direct alkylation of anilines using alcohols via borrowing hydrogen conditions, Chem. Commun. 56 (2020) 13607–13610.

[108] A.A. Khan, A. Ahmad, H.M. Al-Swaidan, S. Haider, M.S. Akhtar, S.U. Khan, Density functional theory study of P-embedded SiC monolayer as a robust metal free catalyst for N_2O reduction and CO oxidation, Mol. Catal. 527 (2022), 112392.

[109] P.J. Silva, New insights into the mechanism of Schiff base synthesis from aromatic amines in the absence of acid catalyst or polar solvents, PeerJ Organ. Chem. 2 (2020), https://doi.org/10.7717/peerj-ochem.4.

[110] J. Bosson, A. Poater, L. Cavallo, S.P. Nolan, Mechanism of racemization of chiral alcohols mediated by 16-electron ruthenium complexes, J. Am. Chem. Soc. 132 (2010) 13146–13149.

[111] L. Hackl, L.P. Ho, D. Bockhardt, T. Bannenberg, M. Tamm, Tetraaminocyclopentadienone iron complexes as hydrogenation catalysts, Organometallics 41 (2022) 836–851.

[112] L. Falivene, V. Barone, G. Talarico, Unraveling the role of entropy in tuning unimolecular vs. bimolecular reaction rates: the case of olefin polymerization catalyzed by transition metals, Mol. Catal. 452 (2018) 138–144.

[113] S. Coufourier, Q. Gaignard-Gaillard, J.-.F. Lohier, A. Poater, S. Gaillard, J.-.L. Renaud, Hydrogenation of CO_2, hydrogenocarbonate, and carbonate to formate in water using phosphine free bifunctional iron complexes, ACS Catal. 10 (2020) 2108–2116.

[114] S. Kozuch, S. Shaik, How to conceptualize catalytic cycles? The energetic span model, Acc. Chem. Res 44 (2011) 101–110.

[115] G.M. Meconi, S.V.C. Vummaleti, J.A. Luque-Urrutia, P. Belanzoni, S.P. Nolan, H. Jacobsen, L. Cavallo, M. Solà, A. Poater, Mechanism of the Suzuki–Miyaura cross-coupling reaction mediated by [Pd(NHC)(allyl)Cl] precatalysts, Organometallics 36 (2017) 2088–2095.

[116] R. Monreal-Corona, A. Díaz-Jiménez, A. Roglans, A. Poater, A. Pla-Quintana, Indolizine synthesis through annulation of pyridinium 1,4-thiolates and copper carbenes: a predictive catalysis approach, Adv. Synth. Catal. 365 (2023) 760–766.

[117] E. Solel, N. Tarannam, S. Kozuch, S. Catalysis, Energy is the measure of all things, Chem. Commun. 55 (2019) 5306–5322.

[118] J.A. Luque-Urrutia, A. Poater, The fundamental non innocent role of water for the hydrogenation of nitrous oxide by PNP pincer Ru-based catalysts, Inorg. Chem. 56 (2017) 14383–14387.

[119] A. Poater, X. Ribas, A. Llobet, L. Cavallo, M. Solà, Complete mechanism of σ* intramolecular aromatic hydroxylation through O_2 activation by a macrocyclic dicopper(I) complex, J. Am. Chem. Soc. 130 (2008) 17710–17717.

[120] M.B. Yeamin, J. Duran, S. Simon, N. Tzouras, S.P. Nolan, A. Poater, Unveiling the complexity of the dual gold(I) catalyzed intermolecular hydroamination of alkynes leading to vinylazoles, Mol. Catal. 518 (2022), 112090.

[121] M. Gimferrer, N. Joly, S. Escayola, E. Viñas, S. Gaillard, M. Solà, J.-.L. Renaud, P. Salvador, A. Poater, Knölker iron catalysts for hydrogenation revisited: non spectator solvent and fine-tuning, Organometallics 41 (2022) 1204–1215.

[122] R. Martínez, D.J. Ramón, M. Yus, Transition-Metal-free indirect friedländer synthesis of quinolines from alcohols, J. Org. Chem. 73 (2008) 9778–9780.